

J. RYŚ * W. RATUSZEK *, M. WITKOWSKA *

COMPARISON OF THE ROLLING TEXTURE FORMATION IN DUPLEX STEELS WITH VARIOUS INITIAL TEXTURES

PORÓWNANIE TWORZENIA SIĘ TEKSTUR WALCOWANIA W STALACH DUPLEX O RÓŻNYCH TEKSTURACH WYJŚCIOWYCH

In the present work the effect of the initial orientation distribution on texture development is analysed in two duplex type steels, X1CrNi24-6 and X4CrNiMo24-6-2, subjected to cold-rolling. Both steels under examination showed very different intensities of the initial textures after the preliminary thermo-mechanical treatment, namely; clearly defined strong textures of ferrite and austenite in steel X1CrNi24-6 and nearly random textures of both constituent phases in the case of steel X4CrNiMo24-6-2.

Comparison of texture formation indicates that essentially both duplex steels show tendency to develop the rolling textures of the constituent phases close to those in single phase steels. In both cases however the process proceeds in different way and the final textures display certain important differences in comparison to the typical ferrite and austenite textures. In the case of the steel with strong initial orientations the formation of the rolling textures consists in spread of the starting textures however the major orientation components in both phases are stable up to high rolling reductions. On the other hand in the steel with random initial orientations a gradual formation of deformation textures is observed in the course of rolling with simultaneous formation of ferrite and austenite bands. It is concluded that in both cases the formation and character of the final deformation textures is strongly influenced by the band-like morphology of two-phase structure.

Prezentowana praca dotyczy analizy wpływu orientacji wyjściowej na rozwój tekstur odkształcenia w dwóch stalach typu duplex, X1CrNi24-6 oraz X4CrNiMo24-6-2, poddanych walcowaniu na zimno. Obie badane stale wykazywały bardzo zróżnicowane intensywności tekstury wyjściowej po wstępnej obróbce cieplno-mechanicznej, tzn. wyraźnie określone silne tekstury ferrytu i austenitu w stali X1CrNi24-6 oraz niemal bezładne tekstury obu składowych faz w przypadku stali X4CrNiMo24-6-2.

Porównanie tworzenia się tekstur wskazuje, że zasadniczo obie stale duplex wykazują tendencje do rozwoju tekstur walcowania obu składowych faz zbliżonych do tych w stalach jednofazowych. Jednak w obydwu przypadkach proces ten zachodzi w odmienny sposób a końcowe tekstury wykazują pewne istotne różnice w porównaniu do typowych tekstur ferrytu i austenitu. W przypadku stali o silnej orientacji wyjściowej tworzenie się tekstur walcowania polega na stopniowym rozmyciu tekstur początkowych, niemniej główne orientacje składowe w obu fazach pozostają stabilne do wysokich odkształceń. Z kolei w stali o bezładnej orientacji wyjściowej w trakcie walcowania obserwuje się stopniowy rozwój tekstur odkształcenia równoległe z tworzeniem pasm ferrytu i austenitu. Stwierdzono, że w obu przypadkach pasmowa morfologia struktury dwufazowej wywiera istotny wpływ na tworzenie się i charakter końcowych tekstur odkształcenia.

1. Introduction

From a number of works it may be concluded that the anisotropic mechanical behaviour of cold-rolled duplex steels is not only the result of a specific morphology of two-phase structure (i.e. grain shape and phase arrangement) but also depends on the crystallographic textures of the constituent phases [1÷5]. That is why the factors affecting the formation of rolling textures in

ferritic-austenitic stainless steels are the subject of major debate (e.g. [4÷13]).

Many reported investigations indicate that a development of deformation textures in duplex type steels depends first of all on the chemical composition. It determines a phase composition of the steel, i.e. the ferrite and austenite volume fractions, as well as the stability of the austenitic γ -phase upon rolling and in consequence a possible contribution of deformation induced ($\gamma \rightarrow \alpha$)

* AGH-UNIVERSITY OF SCIENCE AND TECHNOLOGY, FACULTY OF METALS ENGINEERING AND INDUSTRIAL COMPUTER SCIENCE, AV. MICKIEWICZA 30, 30-059 KRAKÓW, POLAND

phase transformation into the texture development of both constituent phases [5÷10].

It should be noted that deformation mechanisms governing the formation of ferrite and austenite rolling textures in duplex type steels change in comparison to single phase steels because of the presence of the second phase and additionally due to the specific band-like morphology of two-phase structure, which develops in the course of rolling [3÷13].

Another important factors, which are taken into account when analysing texture formation upon cold-rolling of duplex type steels are the initial textures of both constituent phases after thermo-mechanical pre-treatment and deformation conditions (e.g. applied rolling schedules) [6÷13].

The purpose of the present study was comparison of the effect of different initial textures on a development and character of final rolling textures in duplex type ferritic-austenitic steels subjected to cold-rolling within the wide range of deformations. Two extreme cases were examined from the view point of the initial orientation distribution of the constituent phases, namely; clearly defined strong textures of ferrite and austenite in steel X1CrNi24-6 and nearly random textures of both phases in the case of steel X4CrNiMo24-6-2. The phase compositions and the initial morphology of both steels were similar, with the ferritic α -phase constituting the matrix, and the same rolling conditions were applied in both cases.

2. Material and experimental procedure

The materials investigated in the present study were two stainless steels of duplex type, X1CrNi24-6 (steel A) and X4CrNiMo24-6-2 (steel B), with the chemical compositions given in Table I. Phase compositions of both steels were determined by means the metallographic analysis conducted after the solution treatment. The volume fractions of ferrite (V_f) were estimated at about 60% and 65%, for steels A and B respectively. Thus in both cases the ferritic α -phase was more continuous

and constituted the matrix with islands of the austenitic γ -phase. That is way the ferritic-austenitic steels under examination have not a typical duplex structures.

Ingots of both steels were homogenized and then in the case of steel A subjected to forging within the temperature range 1100÷900°C. Afterwards the rectangular steel rods were annealed at the temperature 1100°C for 3÷6 hours and quenched in the water. Subsequent to the preliminary thermo-mechanical treatment the steel rods were subjected to reversed rolling at room temperature within the range up to 90% of thickness reduction. The same rolling conditions were applied for both steels, employing small reductions per pass i.e. the ratio (l_c/h_m) < 0.5, where $l_c = \sqrt{r\Delta h}$ — the length of the arc of contact, r - radius of rolls, Δh — thickness reduction per pass and h_m — the mean thickness of the sheet. In such case the compressive strain does not penetrate the whole thickness of the sheet, hence there is a strain gradient throughout the cross section. In consequence a deformation rate of the centre layer, parallel to the rolling plane, is assumed to be much less than that of the subsurface layers [14].

X-ray investigations were conducted by means of Bruker diffractometer D8 Advance, using Co $K\alpha$ radiation ($\lambda_{K\alpha} = 0,179\text{nm}$). X-ray examination included the texture measurements and the phase analysis from the centre layers of the rolled sheets, for the initial state and after selected rolling reductions. Texture analysis was performed on the basis of the orientation distribution functions (ODFs) calculated from experimental (incomplete) pole figures recorded of three planes for each of the constituent phases, i.e. {110}, {100} and {211} planes for the bcc α -phase and {111}, {100} and {110} planes for the fcc γ -phase. The values of the orientation distribution functions $f(g)$ along the orientation fibres $\alpha_1 = \langle 110 \rangle \parallel \text{RD}$, $\gamma = \langle 111 \rangle \parallel \text{ND}$, $\varepsilon = \langle 001 \rangle \parallel \text{ND}$ for ferrite and $\alpha = \langle 110 \rangle \parallel \text{ND}$, $\eta = \langle 001 \rangle \parallel \text{RD}$, $\tau = \langle 110 \rangle \parallel \text{TD}$ for austenite were thoroughly examined. Simulated transformations of the selected ideal orientations and experimental ODFs were carried out additionally to verify the orientation relation between major components of the ferrite and austenite rolling textures.

TABLE I
Chemical compositions of both duplex type steels under examination (in wt %)

Steel	C	Cr	Ni	Mo	Mn	Si	Al	S	P	N	Fe
A	0.009	23.7	6.0	–	1.23	0.34	< 0.02 0	0.010	<0.008	0.012	bal.
B	0.04	24.3	6.44	1.57	1.29	1.02	0.009	0.013	<0.009	0.014	bal.

The phase composition of both steels, the initial morphology of two-phase structure after the preliminary thermo-mechanical treatment and the formation of ferrite and austenite band-like structure in the course of cold-rolling were analysed by means of optical microscopy.

3. Results and discussion

3.1. Initial texture and structure

Both steels under examination showed very different intensities of the starting textures after the preliminary thermo-mechanical treatment. The occurrence of strong initial textures of both phases was found in steel X1CrNi24-6. Ferrite exhibited the $\{100\}\langle 001\rangle$ cubic texture and the dominant component of the austenite texture was the $\{110\}\langle 001\rangle$ Goss orientation (Fig. 1a).

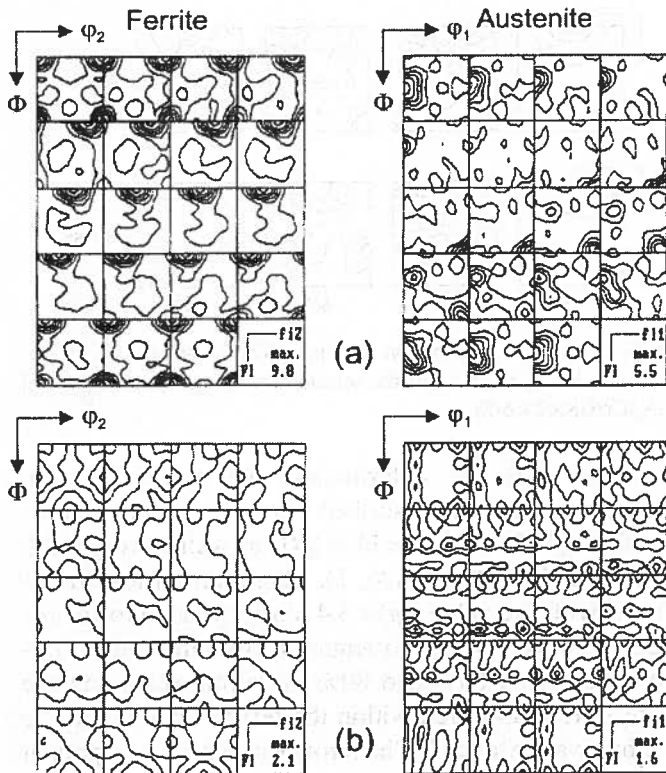


Fig. 1. The starting textures of ferrite and austenite after thermo-mechanical pre-treatment in sections $\varphi_1 = \text{const}$ and $\varphi_2 = \text{const}$ respectively, for steels with strong — (a) and nearly random — (b) orientation distributions

The crystallographic relation between the major texture components of both phases was described by Bain orientation relationship [12, 13]. On the other hand nearly random initial textures of both constituent phases were observed in the case of X4CrNiMo24-6-2 steel. Only relatively weak orientations were found in the ferrite and

austenite textures, namely the $\{110\}\langle 001\rangle$ orientation and the orientation close to the $\{221\}\langle 012\rangle$ respectively (Fig. 1b). It is assumed that the higher values of the orientation distribution function $f(g)$ for ferrite in both cases resulted from the phase compositions of the steels, i.e. the higher volume fractions of the α -phase.

The morphology of the ferrite-austenite structure after the preliminary treatment resulted from the phase composition and the applied type of hot-deformation process. Within the microstructure of both steels, the austenite islands elongated parallel to the main axis were observed on the background of the ferrite matrix on the longitudinal sections of the rods, however on the cross sections the austenite grains were nearly equiaxed. It occurs that after forging of duplex type steels the ferrite-austenite structure exhibits certain degree of anisotropy, however less pronounced in comparison to hot-rolling [4, 8].

3.2. Rolling texture development

Changes of the ferrite and austenite textures during cold-rolling of steel X1CrNi24-6 (A), with strong initial orientations of both constituent phases, are shown in figures 2, 3 and 4, 5 respectively.

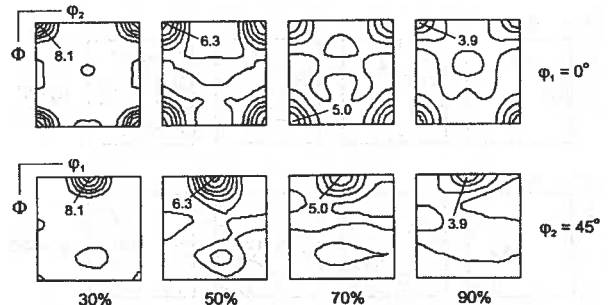


Fig. 2. Orientation distribution functions (ODFs) for ferrite in sections $\varphi_1 = 0^\circ$, $\varphi_2 = 45^\circ$ after the selected rolling reductions — steel A (X1CrNi24-6)

Within the deformation range 30÷90% the strongest component of the ferrite texture was the $\{001\}\langle 100\rangle$ cubic orientation, which is not typical component for the ferrite deformation textures [15,16]. With increasing degree of deformation a considerable decay of the texture intensity was observed, from the value $f(g)=9.8$ for the starting material to $f(g)=3.9$ at 90% of rolling reduction. Very weak orientations ($f(g)=1.5$) from the γ -fibre $\langle 111\rangle\parallel\text{ND}$ appeared not before 90% of reduction (Figs. 2, 3). Within the α_1 -fibre $\langle 110\rangle\parallel\text{RD}$ only weak orientation $\{112\}\langle 110\rangle$ was observed, with the intensity $f(g)$ changing in the course of rolling from 1.2 to 2.7 at 90% of reduction. The $f(g)$ values for orientations from the ε -fibre $\langle 001\rangle\parallel\text{ND}$, including the major cubic component $\{001\}\langle 100\rangle$, decreased with increasing rolling reduction. The rotated cubic orientation $\{001\}\langle 110\rangle$ from

the α_1 - and ε -fibres, which is one of the typical components of ferrite rolling textures [15,16], appeared not before 70% of deformation and remained extremely weak component after 90% of reduction (Figs. 2, 3).

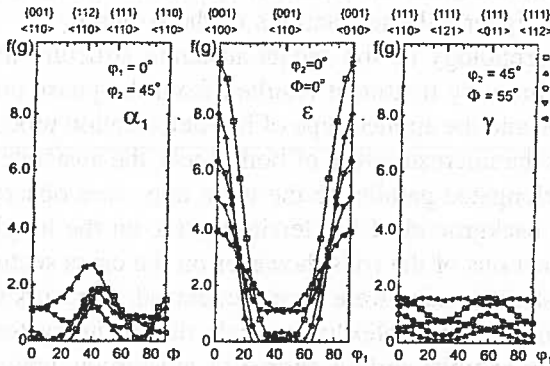


Fig. 3. Values of the orientation distribution function $f(g)$ for ferrite along the orientation fibres; $\alpha_1 = \langle 110 \rangle \parallel \text{RD}$, $\varepsilon = \langle 001 \rangle \parallel \text{ND}$ and $\gamma = \langle 111 \rangle \parallel \text{ND}$ - steel A (X1CrNi24-6)

Dominant component of the austenite rolling texture within the whole range of deformations was the Goss orientation $\{110\}\langle 001 \rangle$, which belonged to the limited fibres $\alpha = \langle 110 \rangle \parallel \text{ND}$ and $\eta = \langle 001 \rangle \parallel \text{RD}$ (Figs. 4,5).

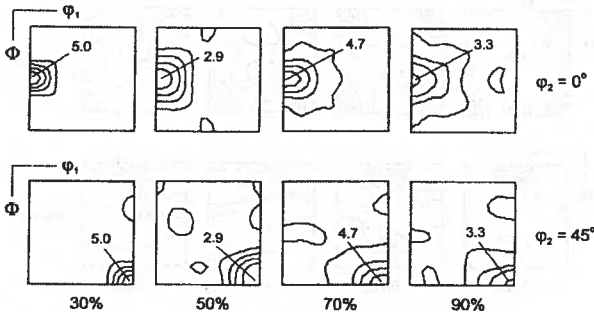


Fig. 4. Orientation distribution functions (ODFs) in sections $\varphi_1 = 0^\circ$, $\varphi_2 = 45^\circ$ for austenite after the selected rolling reductions — steel A (X1CrNi24-6)

With increasing rolling reduction the significant decrease of the intensity was observed for the major component $\{110\}\langle 001 \rangle$, from $f(g)=5.5$ for the starting material to $f(g)=3.3$ at 90% of deformation, with simultaneous elongation of the α - and η -fibres. The alloy-type orientation $\{110\}\langle 112 \rangle$, from the α - and β -fibres, appeared only at high deformations having the $f(g)$ values of 1.4 and 1.3 at 70% and 90% of reduction respectively. Moreover in the whole range of deformations the $\{552\}\langle 115 \rangle$ orientation from the τ -fibre $\langle 110 \rangle \parallel \text{TD}$ was observed as well as relatively weak component $\{113\}\langle 332 \rangle$. Very weak copper-type orientation $\{112\}\langle 111 \rangle$ appeared only at 50% of reduction as well as the S-type orientation $\{213\}\langle 364 \rangle$ from the β -fibre, which was observed only after 90% of deformation.

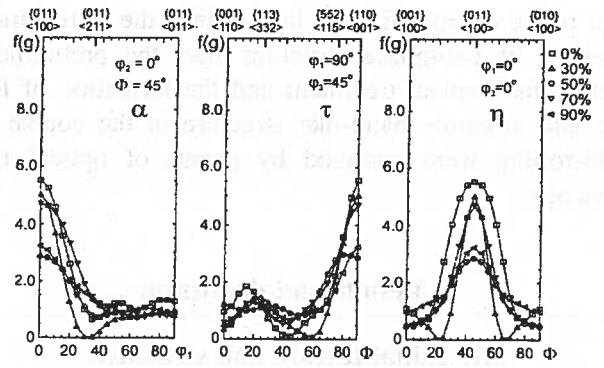


Fig. 5. Values of the orientation distribution function $f(g)$ for austenite along the orientation fibres; $\alpha = \langle 110 \rangle \parallel \text{ND}$, $\tau = \langle 110 \rangle \parallel \text{TD}$ and $\eta = \langle 001 \rangle \parallel \text{RD}$ — steel A (X1CrNi24-6)

The formation of ferrite and austenite textures upon rolling of steel X4CrNiMo24-6-2 (B), with nearly random initial orientations of both constituent phases, is shown in figures 6, 7 and 8, 9 respectively.

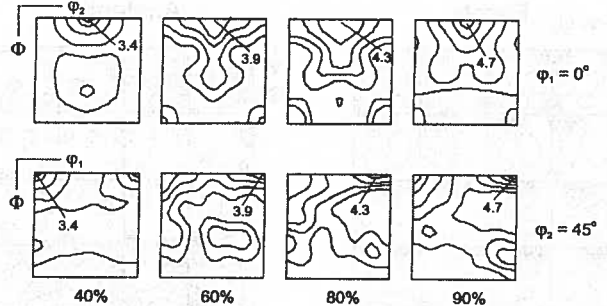


Fig. 6. Orientation distribution functions (ODFs) for ferrite in sections $\varphi_1 = 0^\circ$, $\varphi_2 = 45^\circ$ after the selected rolling reductions — steel B (X4CrNiMo24-6-2)

After 40% of deformation the rolling texture of ferrite may be described by the limited fibres $\varepsilon = \langle 001 \rangle \parallel \text{ND}$ and $\alpha_1 = \langle 110 \rangle \parallel \text{RD}$ as well as very weak γ -fibre $\langle 111 \rangle \parallel \text{ND}$ (Figs. 6, 7). Maximum of texture intensity, with the value $f(g)=3.4$, corresponded to the rotated cubic $\{001\}\langle 110 \rangle$ orientation from the limited α_1 - and ε -fibres. At 60% and 80% of rolling reduction the entire ε -fibre appeared within the ferrite texture and the α_1 -fibre was extended. The strongest texture component after 60% of deformation remained the $\{001\}\langle 110 \rangle$ orientation, having the value $f(g)=3.9$ (Figs. 6, 7). However at 80% of reduction the texture maximum ($f(g)=4.3$) was shifted towards the $\{001\}\langle 320 \div 210 \rangle$ orientation range. While the γ -fibre was somewhat strengthened after 60% it practically disappeared at 80% of reduction. After 90% of deformation the texture of ferrite was slightly sharper, with the maximum value $f(g)=4.7$ corresponding again to the rotated cubic $\{001\}\langle 110 \rangle$ orientation. Both orientation fibres describing the final rolling texture of ferrite, i.e. the α_1 - and ε -fibres were strongly inhomogeneous and practically limited. Very weak γ -fibre also

appeared within the final texture and extended from the $\{111\}\langle 110 \rangle$ orientation to the $\{111\}\langle 112 \rangle$ one (Figs. 6, 7).

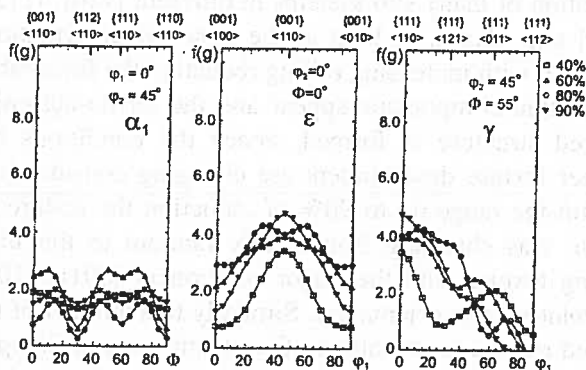


Fig. 7. Values of the orientation distribution function $f(g)$ for ferrite along the orientation fibres; $\alpha = \langle 110 \rangle \parallel \text{RD}$, $\epsilon = \langle 001 \rangle \parallel \text{ND}$ and $\gamma = \langle 111 \rangle \parallel \text{ND}$ — steel B (X4CrNiMo24-6-2)

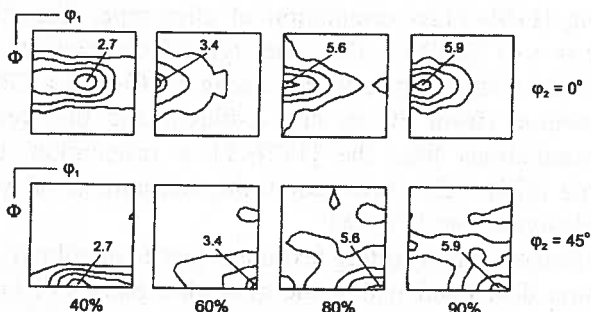


Fig. 8. Orientation distribution functions (ODFs) in sections $\phi_2 = 0^\circ$, $\phi_2 = 45^\circ$ for austenite after the selected rolling reductions — steel B (X4CrNiMo24-6-2)

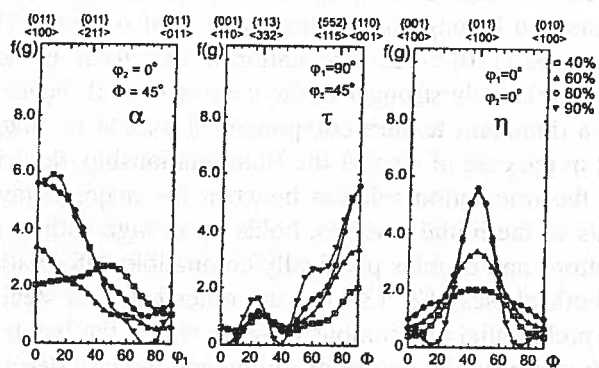


Fig. 9. Values of the orientation distribution function $f(g)$ for austenite along the orientation fibres; $\alpha = \langle 110 \rangle \parallel \text{ND}$, $\tau = \langle 110 \rangle \parallel \text{TD}$ and $\eta = \langle 001 \rangle \parallel \text{RD}$ — steel B (X4CrNiMo24-6-2)

The rolling texture of austenite at 40% of deformation describe the inhomogeneous α -fibre and the limited η -fibre. The strongest texture component was the orientation close to the $\{110\}\langle 111 \rangle$ from the α -fibre, with the value $f(g)=2.7$. Relatively high texture intensities, $f(g)=2.4$ and 2.0 , had also the $\{110\}\langle 112 \rangle$ and

$\{110\}\langle 001 \rangle$ orientations respectively (Figs. 8, 9). At higher deformation degrees the α -fibre was strongly limited. The maximum of texture intensity after 60% and 80% of rolling reduction was shifted towards the $\{110\}\langle 001 \rangle$ Goss orientation, having the $f(g)$ values 3.4 and 5.6 respectively. After 90% of deformation the strongest texture component was the $\{110\}\langle 115 \rangle$ orientation ($f(g)=5.9$) from the limited α -fibre, which extended within the $\{110\}\langle 001 \rangle \div \{111\}$ orientation range. Apart of it relatively strong orientations within the austenite rolling texture were the $\{110\}\langle 001 \rangle$ Goss orientation ($f(g)=5.4$), the $\{110\}\langle 113 \rangle$ orientation ($f(g)=3.9$) and the alloy-type $\{110\}\langle 112 \rangle$ orientation ($f(g)=3.5$). With increasing deformation contribution of the $\{552\}\langle 115 \rangle$ orientation was also observed. Moreover the orientations of $\{113\}\langle 332 \rangle$ type and the S orientation appeared at 90% of rolling reduction (Figs. 8, 9).

3.3. Comparison of rolling textures

In the course of rolling deformation of two-phase ferritic-austenitic steels the flow behaviour of the constituent phases is usually different in comparison to single phase steels. The basic reason is the interaction of both α - and γ -phases and the formation of a specific band-like morphology of two-phase structure, which consists of alternated ferrite and austenite layers parallel to the rolling plane (Fig. 10 a,b). In such circumstances the conditions for the texture formation are substantially changed and hence the frequently observed differences between the rolling textures of the α - and γ -phases in duplex steels and the rolling textures of single phase ferritic or austenitic steels [6÷13].

In the case of both duplex type steels under examination the major differences concern especially the development and the character of the rolling textures in the ferritic α -phases.

As frequently reported, a fiber-type texture in single phase bcc steels develops because slip is possible on several slip planes, i.e.; $\{110\}$, $\{112\}$, and $\{123\}$. Usually the dominant components within the rolling textures of low-carbon steels and chromium stainless steels are the orientations; $\{001\}\langle 110 \rangle$, $\{112\}\langle 110 \rangle$ and $\{111\}\langle 110 \rangle$ from the α_1 -fibre $\langle 110 \rangle \parallel \text{RD}$ as well as $\{111\}\langle 110 \rangle$ and $\{111\}\langle 112 \rangle$ from the γ -fibre $\langle 111 \rangle \parallel \text{ND}$ [15, 16]. However, in contrast to this, it has been often observed that no typical α_1 -fiber or γ -fibre develop in the ferritic phase of duplex stainless steels during rolling. Instead, the texture is composed of ideal components with the rotated cube $\{001\}\langle 110 \rangle$ as the dominant one [1÷7].

In the case of steel A, with strong initial orientations in both constituent phases, the character of developed ferrite rolling texture is also completely different

in comparison to single phase steels. The major component from the ferrite initial texture, i.e. the $\{100\}\langle 001\rangle$ cubic orientation, is stable up to high rolling reductions in spite of the fact that this is not a typical orientation of ferrite rolling textures [15, 16]. Additionally the rolling texture of ferrite does not exhibit a fibre character and the $\{100\}\langle 001\rangle$ orientation remained the dominant texture component on every stage of deformation (Figs. 2, 3). Essentially the formation of the final rolling texture in the ferritic phase of steel A consists in the spread of the strong and sharp initial texture. Such behaviour is the result of a number of factors. First of all, from the very beginning, the strong initial orientation of ferrite forces operation of only certain most stressed $\{100\}\langle 111\rangle$ slip systems in a major part of grains. Moreover, the initial texture of ferrite, which is related with the austenite texture through the Bain orientation relationship, enables plastically compatible deformation of both constituent phases. Detailed analysis of this aspect is given by the present authors elsewhere [12, 13]. Additionally, the band-like morphology of the ferrite and austenite structure as well as the applied rolling schedule employing small reductions per pass, both of which restrain significant lattice rotations and in consequence confine considerable orientation changes within the centre layers of the rolled sheets.

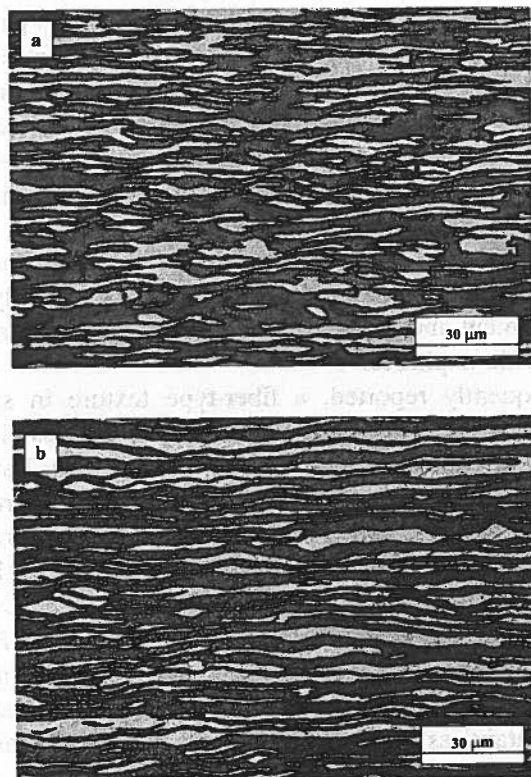


Fig. 10. Ferrite-austenite banded structure in cold-rolled duplex type steels on the longitudinal section (ND-RD); (a) steel X1CrNi24-6, 70% of reduction and (b) steel X4CrNiMo24-6-2, 80% of reduction

On the other hand, conditions for the rolling texture formation within the ferritic phase of steel B are different due to the nearly random initial texture, which enables operation of many slip systems in different $\{110\}$, $\{112\}$, $\{123\}$ slip planes, at least at the onset of deformation. However with increasing rolling reduction the favourable orientation components appear and the ferrite-austenite layered structure is formed, hence the conditions for further texture development are changing considerably. Within the range up to 90% of reduction the texture of ferrite was changing from nearly random to the final rolling texture with the major component $\{001\}\langle 110\rangle$, i.e. rotated cube orientation. Similarly to a number of reported results, practically no fiber texture was developed within the ferritic phase of steel B, since the α_1 - and ε -fibres are limited and the γ -fibre is extremely weak (Figs. 6, 7).

Rolling textures of austenitic steels, with relatively low stacking fault energy, are usually described by strong $\{110\}\langle 112\rangle$ orientation of alloy-type, from the fibre $\alpha = \langle 110\rangle \parallel \text{ND}$. The other typical components of austenite textures include the strong $\{110\}\langle 001\rangle$ Goss orientation (from the η - and α -fibres) and the weaker orientations like; the $\{112\}\langle 111\rangle$ orientation, the S-type $\{123\}\langle 523\rangle$ orientation, the orientations of type $\{111\}\langle uvw\rangle$, etc [17, 18].

Rather similar rolling textures, close to an alloy-type texture, developed within the austenitic phases of both duplex steels under examination (Figs. 4, 5 and 8, 9). The strongest components of the final rolling textures are; the $\{110\}\langle 001\rangle$ Goss orientation in steel A and the orientation $\{110\}\langle 115\rangle$ close to the $\{110\}\langle 001\rangle$ one in the case of steel B. In both cases the $\{110\}\langle 001\rangle$ Goss orientation belongs to the limited η - and α -fibres. The alloy-type $\{110\}\langle 112\rangle$ orientation is very weak in steel A and relatively stronger in the case of steel B, hence is not a dominant texture component. It should be noted, that in the case of steel A the Bain relationship, describing the orientation relation between the major components of the initial textures, holds up to high rolling reductions and enables plastically compatible deformation of both phases [12, 13]. On the other hand, in steel B the preferential orientations develop within the bands of both phases in the course of rolling and the best description of the orientation relation between the ferrite and austenite texture components gives the Kurdjumov-Sachs relationship.

The results of the phase analysis and the texture measurements for both examined steels do not indicate at any significant role of deformation induced ($\gamma \rightarrow \alpha$) phase transformation and its contribution into the texture development of constituent phases.

4. Concluding remarks

Comparison of texture formation in two cold-rolled duplex type steels, with very different initial orientation distributions, indicates that regardless of whether the constituent phases exhibit strong (steel A) or random (steel B) initial textures, the rolling texture development differs from that in single phase steels. The major differences concern especially the character of the ferrite rolling textures and rather low texture intensities of constituent phases in both steels.

For the case of the steel A with strong initial textures in both constituent phases, i.e. the $\{100\}\langle 001\rangle$ cubic texture of ferrite and the strong $\{110\}\langle 001\rangle$ Goss component in the austenite texture, the formation of the final rolling textures consists in spread of the starting texture components. However the major orientations in both phases are stable and dominant up to high rolling reductions and the textures of both phases do not exhibit a fibre character.

In steel B, with random initial orientations of both constituent phases, a gradual formation of deformation textures is observed in the course of rolling with simultaneous formation of ferrite and austenite bands. The strongest components of the final rolling textures are the $\{001\}\langle 110\rangle$ rotated cubic orientation in the ferrite texture and the component close to the $\{110\}\langle 001\rangle$ Goss orientation in the austenite texture. Also for the case of steel B the final textures of both phases practically do not exhibit a fibre character typical for single phase steels.

The rolling texture formation of the ferritic α -phases strongly differs from each other depending on the initial orientation distribution and in both cases reveals certain differences in comparison to single phase ferritic steels. The austenitic γ -phases of both examined duplex type steels developed similar deformation textures, close to an alloy-type rolling texture, which is typical for single phase materials with low stacking fault energy.

Irrespective of the initial orientation distribution the formation and character of the final deformation textures in both steels is strongly influenced by the specific morphology of the ferrite and austenite structure formed in the course of rolling. The band-like two-phase structure reduces significant lattice rotations and changes deformation behaviour of both constituent phases. In consequence it confines a spread and subsequent changes of the strong initial textures of the constituent phases in the case of the steel A and restrains a development of typical rolling textures within the ferrite and austenite bands in the case of steel B.

Acknowledgements

The work was supported by the Polish Committee for Scientific Research (KBN) under the contract No. 11.11.110.712.

REFERENCES

- [1] W.B. Hutchinson, K. Ushioda, G. Runnsjö, Anisotropy of Tensile Behaviour in a Duplex Stainless Steel Sheet, *Mater. Science and Techn.* **1**, 728 (1985).
- [2] W.B. Hutchinson, U. Von Schlippenbach, J. Jonsson, Textures and Anisotropy in Duplex Stainless Steel SS 23477, *Proc. Duplex Stainless Steels'86*, Netherlands 326 -330, (1986).
- [3] J.J. Moverare, M. Oden, Influence of Elastic and Plastic Anisotropy on the Flow Behaviour in a Duplex Stainless Steel, *Metall. and Mater. Trans.* **33 A**, 57 (2002).
- [4] A. Ul-Haq, H. Weiland, H.-J. Bunge, Textures and Microstructures in Duplex Stainless Steel, *Mater. Science and Techn.* **10**, 289 (1994).
- [5] N. Akdut, J. Foct, Phase Boundaries and Deformation in High Nitrogen Duplex Stainless Steels, I.- Rolling Texture Development, II.- Analysis of Deformation Mechanisms by Texture Measurements, *Scripta Metall. et Mater.* **32**, 103 & 109 (1995).
- [6] N. Akdut, J. Foct, G. Gottstein, Cold Rolling Texture Development of (α/γ) Duplex Stainless Steel, *Steel Research* **67**, 450 (1996).
- [7] N. Akdut, J. Foct, Microstructure and Deformation Behaviour of High Nitrogen Duplex Stainless Steel, *ISIJ International*. **36**, 883 (1996).
- [8] J. Keichel, J. Foct, G. Gottstein, Deformation and Annealing Behavior of Nitrogen Alloyed Duplex Stainless Steels. Part I: Rolling, *ISIJ International*. **43**, 1781 (2003).
- [9] J. Ryś, W. Ratuszek, J. Woźniak, K. Chruściel, Tekstura i struktura stali austenityczno-ferrytycznej typu duplex po odkształceniu plastycznym na zimno, *Inż. Mater.* **XX**, 6, 601 (1999).
- [10] W. Ratuszek, J. Ryś, K. Chruściel, Texture Development in Cold-rolled Austenitic-Ferritic Steel, *Proc. 12-th ICOTOM*, Canada, p. 1071 (1999).
- [11] W. Ratuszek, J. Ryś, K. Chruściel, Effect of Deformation Mode on Texture Development in Cold-rolled Duplex Steel, *Archives of Metallurgy* **44**, 305 (1999).
- [12] J. Ryś, W. Ratuszek, M. Witkowska, The Effect of Initial Orientation and Rolling Schedule on Texture Development in Duplex Steel, *Materials Science Forum* **495-497**, 375-380 (2005).
- [13] J. Ryś, W. Ratuszek, M. Witkowska, Rolling Texture Development in Duplex Type Steel with Strong Initial Texture, *Archives of Metallurgy and Materials* **50**, 857-870 (2005).
- [14] A. Tselikov, *Stress and Strain in Metal Rolling*, Mir Publishers, Moscow (1967).
- [15] K. Lücke, M. Hölscher, Rolling and Recrystallization Textures of BCC Steels, *Textures and Microstructures* **14-18**, 585 (1991).
- [16] D. Raabe, K. Lücke, Textures of Ferritic Stainless Steels, *Mater. Science and Techn.* **9**, 302 (1993).

[17] C. Donadille, R. Valle, P. Dervin, R. Penelle, Development of Texture and Microstructure During Cold-Rolling and Annealing of fcc Alloys: Example of an Austenitic Stainless Steel, *Acta Metall.* **37**, 1547 (1989).

Received: 20 February 2006.

[18] D. Raabe, Texture and Microstructure Evolution during Cold Rolling of a Strip Cast and of a Hot Rolled Austenitic Stainless Steel, *Acta Materialia* **45**, 1137 (1997).

...the texture evolution during cold rolling of a strip cast and of a hot rolled austenitic stainless steel. The texture evolution is characterized by the evolution of the intensity of the $\{111\}$ and $\{110\}$ reflections. The texture evolution is characterized by the evolution of the intensity of the $\{111\}$ and $\{110\}$ reflections. The texture evolution is characterized by the evolution of the intensity of the $\{111\}$ and $\{110\}$ reflections.

...the texture evolution during cold rolling of a strip cast and of a hot rolled austenitic stainless steel. The texture evolution is characterized by the evolution of the intensity of the $\{111\}$ and $\{110\}$ reflections. The texture evolution is characterized by the evolution of the intensity of the $\{111\}$ and $\{110\}$ reflections. The texture evolution is characterized by the evolution of the intensity of the $\{111\}$ and $\{110\}$ reflections.

...the texture evolution during cold rolling of a strip cast and of a hot rolled austenitic stainless steel. The texture evolution is characterized by the evolution of the intensity of the $\{111\}$ and $\{110\}$ reflections. The texture evolution is characterized by the evolution of the intensity of the $\{111\}$ and $\{110\}$ reflections. The texture evolution is characterized by the evolution of the intensity of the $\{111\}$ and $\{110\}$ reflections.

...the texture evolution during cold rolling of a strip cast and of a hot rolled austenitic stainless steel. The texture evolution is characterized by the evolution of the intensity of the $\{111\}$ and $\{110\}$ reflections. The texture evolution is characterized by the evolution of the intensity of the $\{111\}$ and $\{110\}$ reflections. The texture evolution is characterized by the evolution of the intensity of the $\{111\}$ and $\{110\}$ reflections.

...the texture evolution during cold rolling of a strip cast and of a hot rolled austenitic stainless steel. The texture evolution is characterized by the evolution of the intensity of the $\{111\}$ and $\{110\}$ reflections. The texture evolution is characterized by the evolution of the intensity of the $\{111\}$ and $\{110\}$ reflections. The texture evolution is characterized by the evolution of the intensity of the $\{111\}$ and $\{110\}$ reflections.

Addressing

The authors are grateful to the DLR (German Research Aerospace Establishment) for financial support.